

5/3-27

N89-13655

181381
158

DETERMINING BONDING, THICKNESS, AND DENSITY
VIA THERMAL WAVE IMPEDANCE NDE

D. R. Green
Westinghouse Hanford Company
Richland, Washington 99352

Bonding, density, and thickness of coatings have a vital effect on their performance in many applications. Pioneering development work by the author on thermal wave nondestructive evaluation (NDE) methods during the past 25 years has resulted in an array of useful techniques for performing bonding, density, and thickness measurements in a practical shop environment. The most useful thermal wave methods for this purpose are based on thermal wave surface impedance measurement or scanning. A pulse of heat from either a thermal transducer or a hot gas pulse is projected onto the surface, and the resulting temperature response is analyzed to unfold the bonding, density, and thickness of the coating. An advanced emissivity independent infrared method has been applied to detect the temperature response. These methods have recently been completely computerized and can automatically provide information on coating quality in near real-time using the proper equipment. Complex shapes such as turbine blades can be scanned. Microscopic inhomogeneities such as microstructural differences and small, normal, isolated voids do not cause problems but are seen as slight differences in the bulk thermal properties. Test objects with rough surfaces can be effectively nondestructively evaluated using proper thermal surface impedance methods. No contact with the test object is required, and no couplants or other contaminants are used. Thermal wave NDE might be called a "Wave of the Future", as well as a "Wave at the Past". Recent work done on thermal wave NDE by independent groups in the U.S., as well as abroad, has confirmed the potential of some of these methods for practical coating NDE applications. Some of the basic principles involved, as well as metallographic results illustrating the ability of the thermal wave surface impedance method to detect natural nonbonds under a two-layer thermally sprayed coating, will be presented in this paper.

PRECEDING PAGE BLANK NOT FILMED

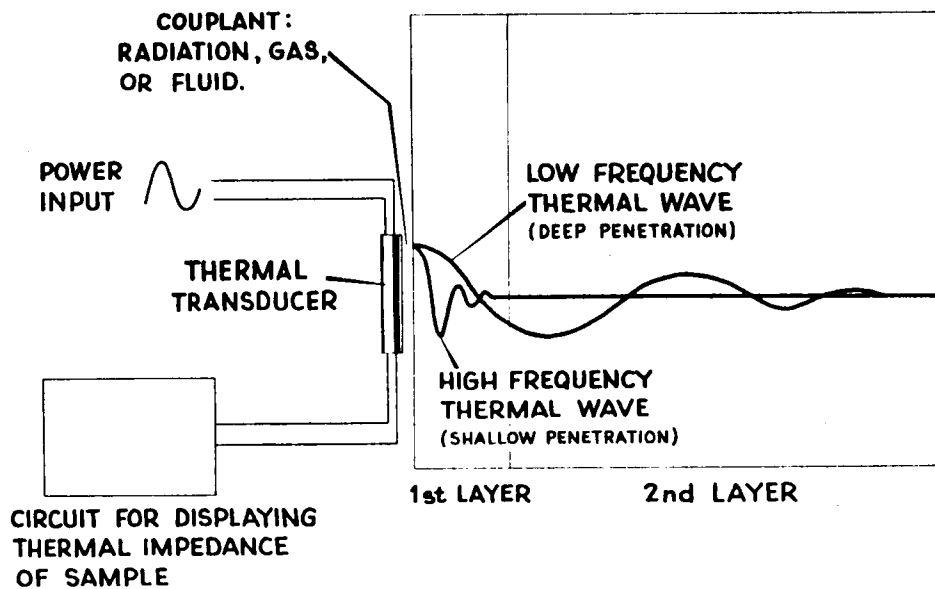
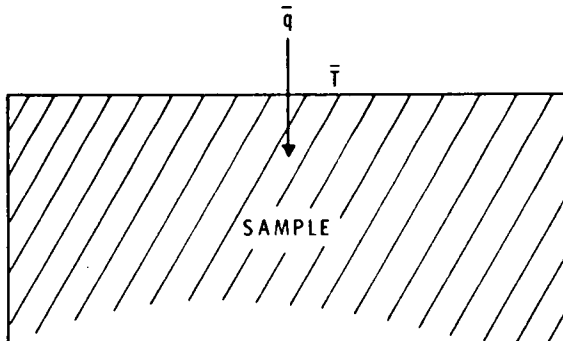


Figure 1.



FOR SINUSOIDAL \bar{q} AND \bar{T} , THE THERMAL SURFACE IMPEDANCE IS DEFINED AS

$$Z = \left[\frac{\bar{T}}{\bar{q}} \right]_{x=0}$$

Figure 2.

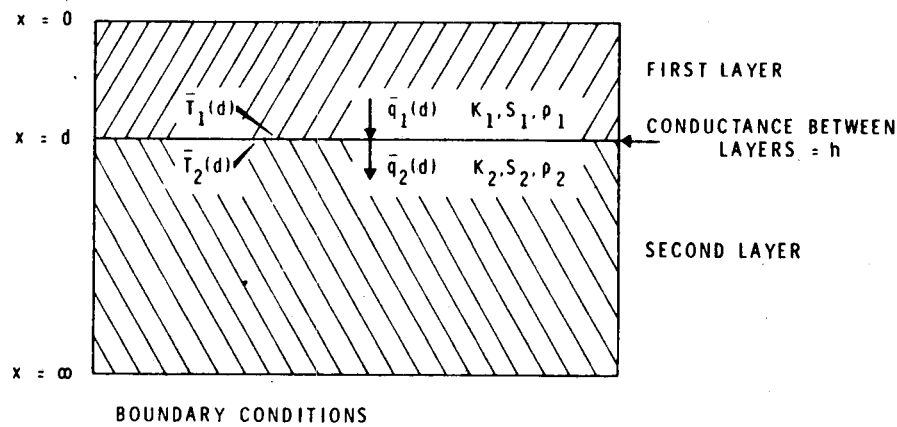
$$\text{Heat Flow, } q = C e^{-(1-j)x/\delta} \quad (1)$$

$$\text{Penetration Depth, } \delta = \sqrt{\frac{K}{\pi f S \rho}} \quad (2)$$

$$\text{Surface Thermal Impedance, } Z = [T/q]_{x=0} \quad (3)$$

Figure 3.

ORIGINAL PAGE IS
OF POOR QUALITY



BOUNDARY CONDITIONS

$$\lim_{x \rightarrow \infty} \bar{q} = 0$$

$$x \rightarrow \infty$$

$$\bar{q}_1(d) = \bar{q}_2(d)$$

$$\bar{T}_1(d) = \bar{T}_2(d) + \frac{\bar{q}_2(d)}{h}$$

Figure 4.

THERMAL SURFACE IMPEDANCE FOR A LAYER IN GOOD CONTACT WITH A SEMI-INFINITE SECOND LAYER

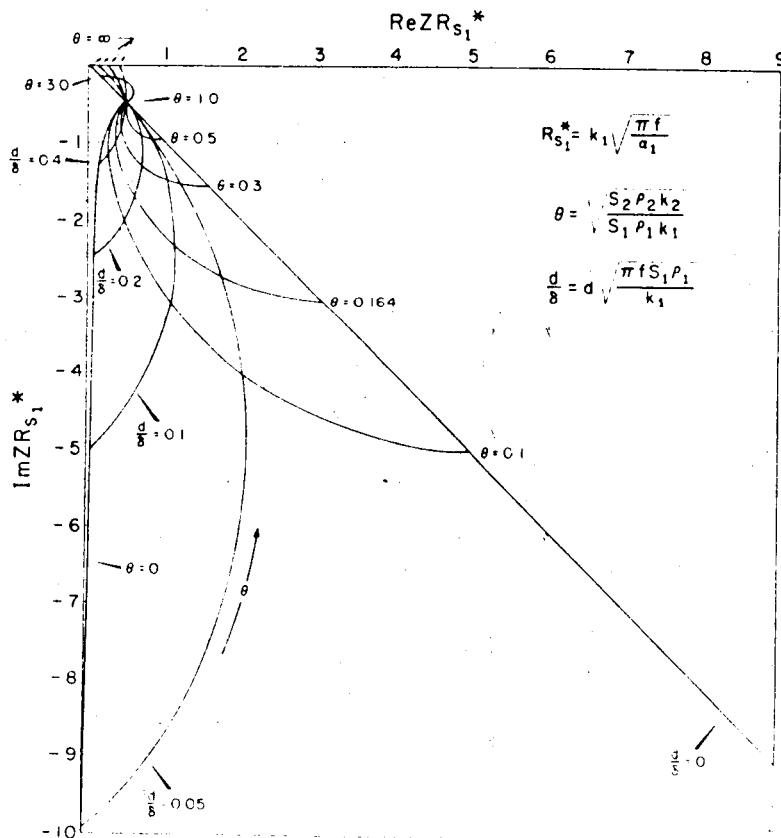


Figure 5.

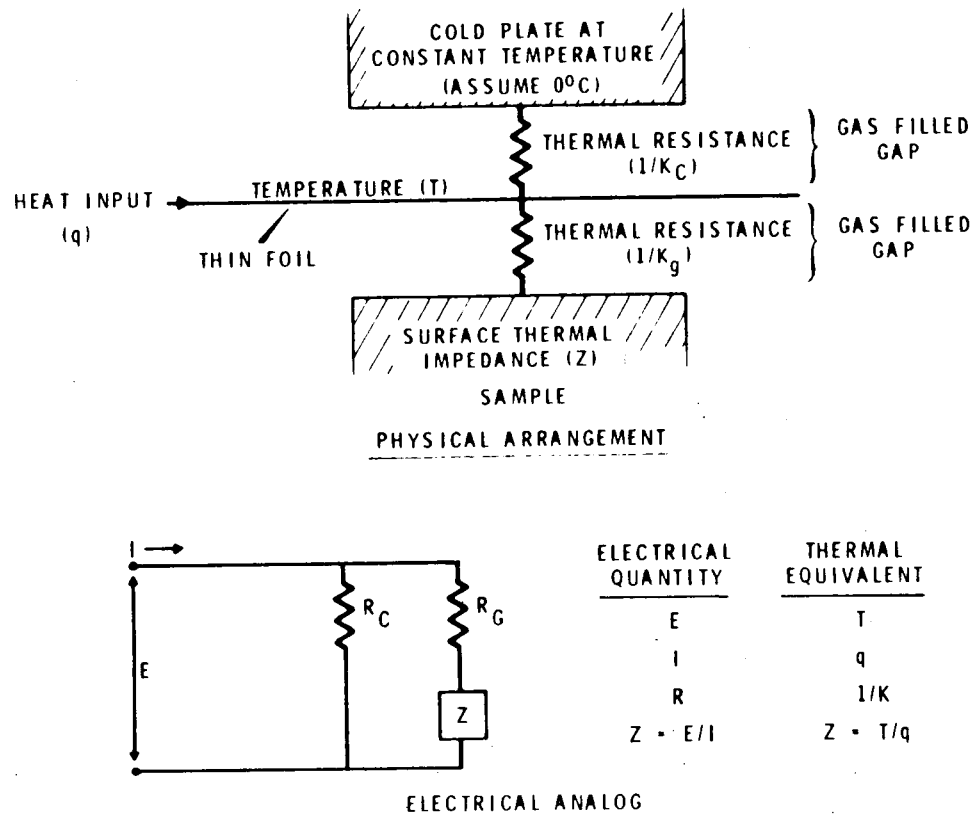
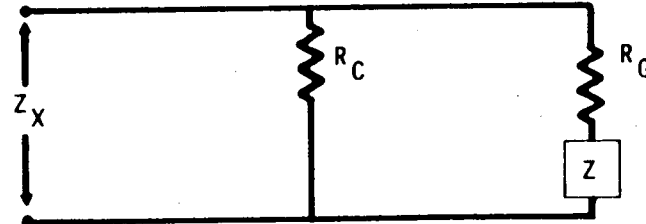


Figure 6.

RELATIONSHIP BETWEEN THERMAL INPUT
IMPEDANCE OF TRANSDUCER, AND THERMAL
SURFACE IMPEDANCE OF SAMPLE



$$\frac{1}{Z_X} = \frac{1}{R_C} + \frac{1}{R_G + Z}$$

HENCE

$$Z = \frac{R_C Z_X}{R_C - Z_X} - R_G$$

AND

$$Z_X = \frac{R_C(R_G + Z)}{R_C + R_G + Z}$$

Figure 7.

BLOCK DIAGRAM OF THE SINUSOIDAL THERMAL WAVE TESTER

ORIGINAL PAGE IS
OF POOR QUALITY

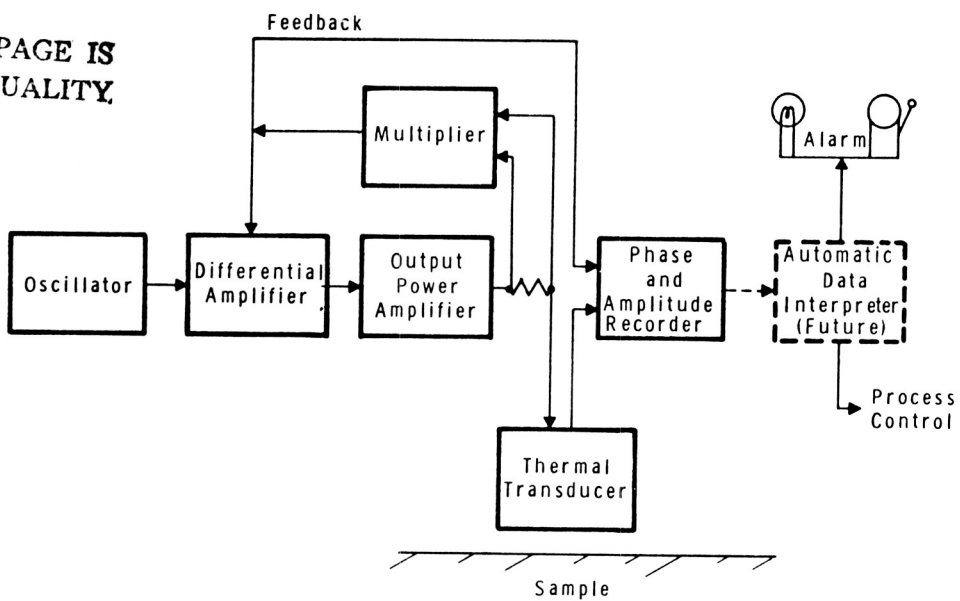


Figure 8.

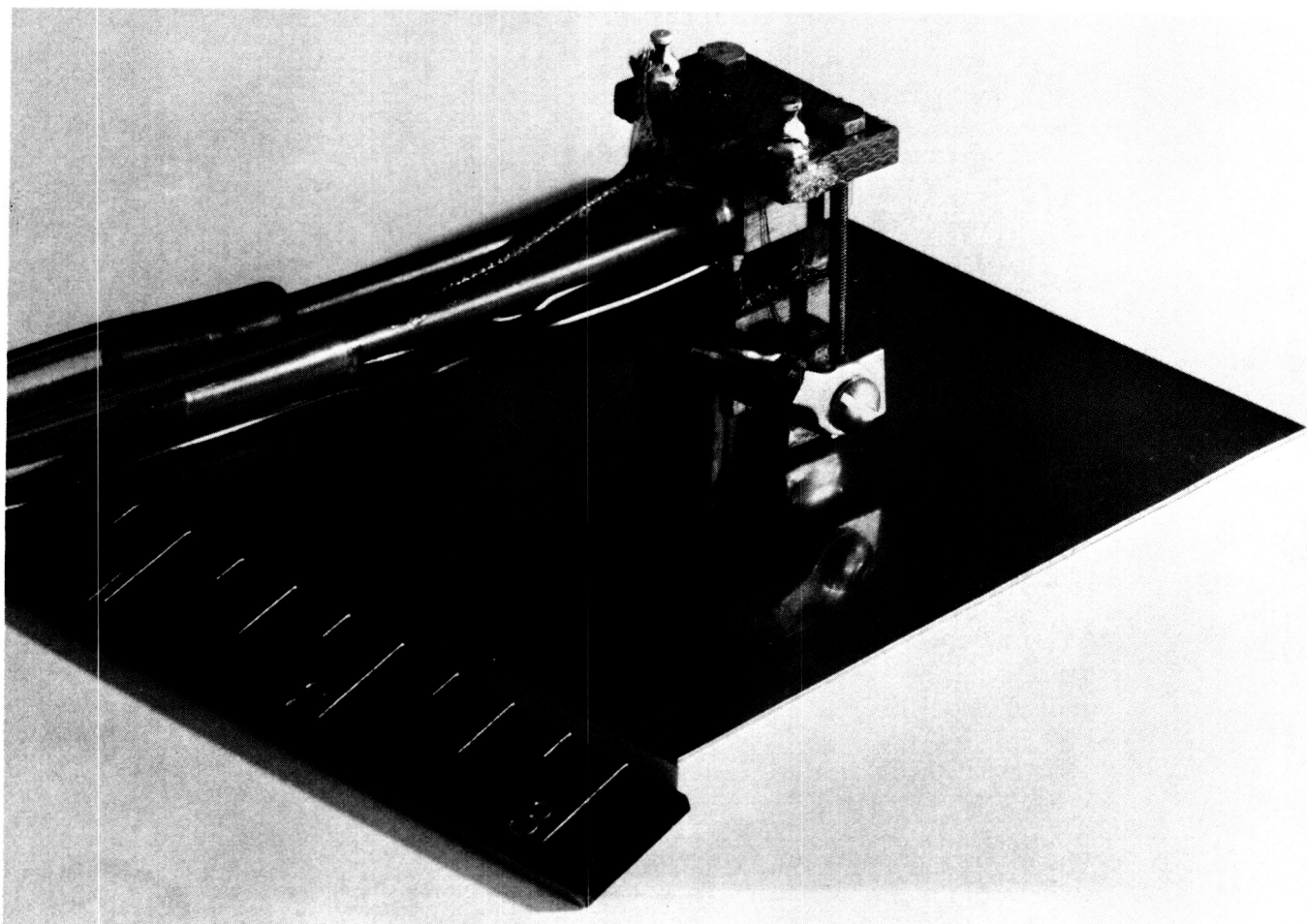


Figure 9.

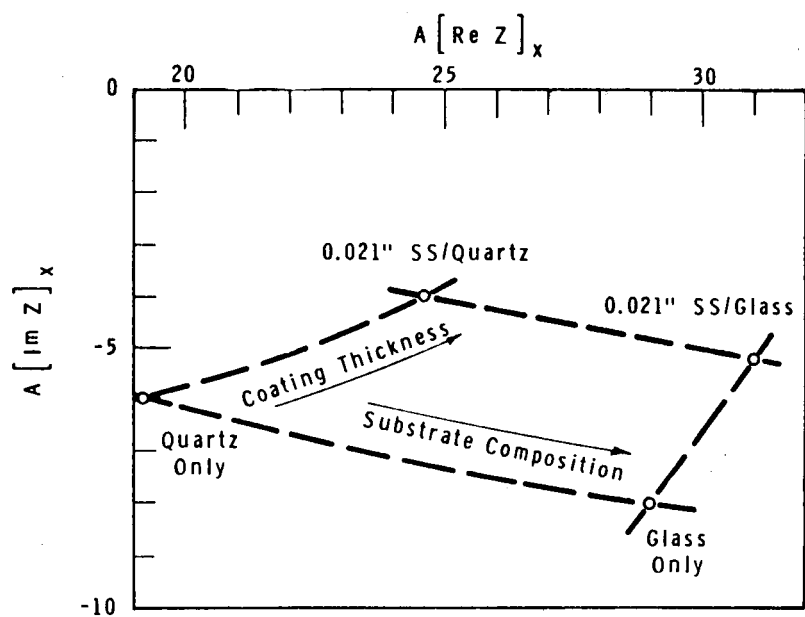


Figure 10.

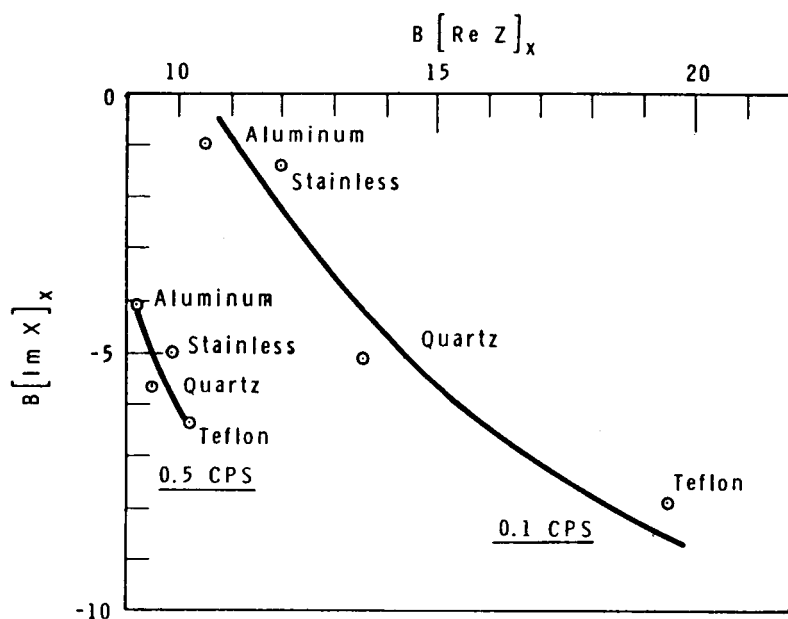


Figure 11.

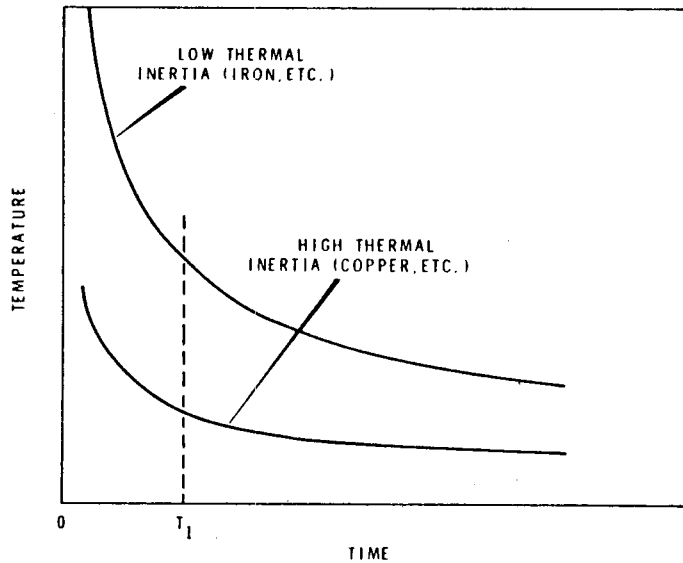


Figure 12.

$$\mathcal{L} \left\{ \frac{f(t)}{y(t)} \right\} = Z(\bar{p})$$

THEN, FROM THE DEFINITION OF THE LAPLACE TRANSFORM,

$$\mathcal{L} \{ f(t) \} = \int_0^{\infty} e^{-\bar{p}t} f(t) dt$$

$$\mathcal{L} \{ y(t) \} = \int_0^{\infty} e^{-\bar{p}t} y(t) dt$$

WHEN $f(t)$ AND $y(t)$ CONVERGE SO THAT THESE TWO INTEGRALS ARE BOUNDED AFTER REPLACING \bar{p} BY $j\omega$, WE CAN WRITE:

$$\begin{aligned} \mathcal{L} \{ f(t) \} &= \int_0^{\infty} e^{-j\omega t} f(t) dt \\ &= \int_0^{\infty} f(t) \cos \omega t dt - j \int_0^{\infty} f(t) \sin \omega t dt \end{aligned}$$

AND

$$\begin{aligned} \mathcal{L} \{ y(t) \} &= \int_0^{\infty} e^{-j\omega t} y(t) dt \\ &= \int_0^{\infty} y(t) \cos \omega t dt - j \int_0^{\infty} y(t) \sin \omega t dt \end{aligned}$$

AND HENCE,

$$Z(j\omega) = \frac{\int_0^{\infty} f(t) \cos \omega t dt - j \int_0^{\infty} f(t) \sin \omega t dt}{\int_0^{\infty} y(t) \cos \omega t dt - j \int_0^{\infty} y(t) \sin \omega t dt}$$

Figure 13.

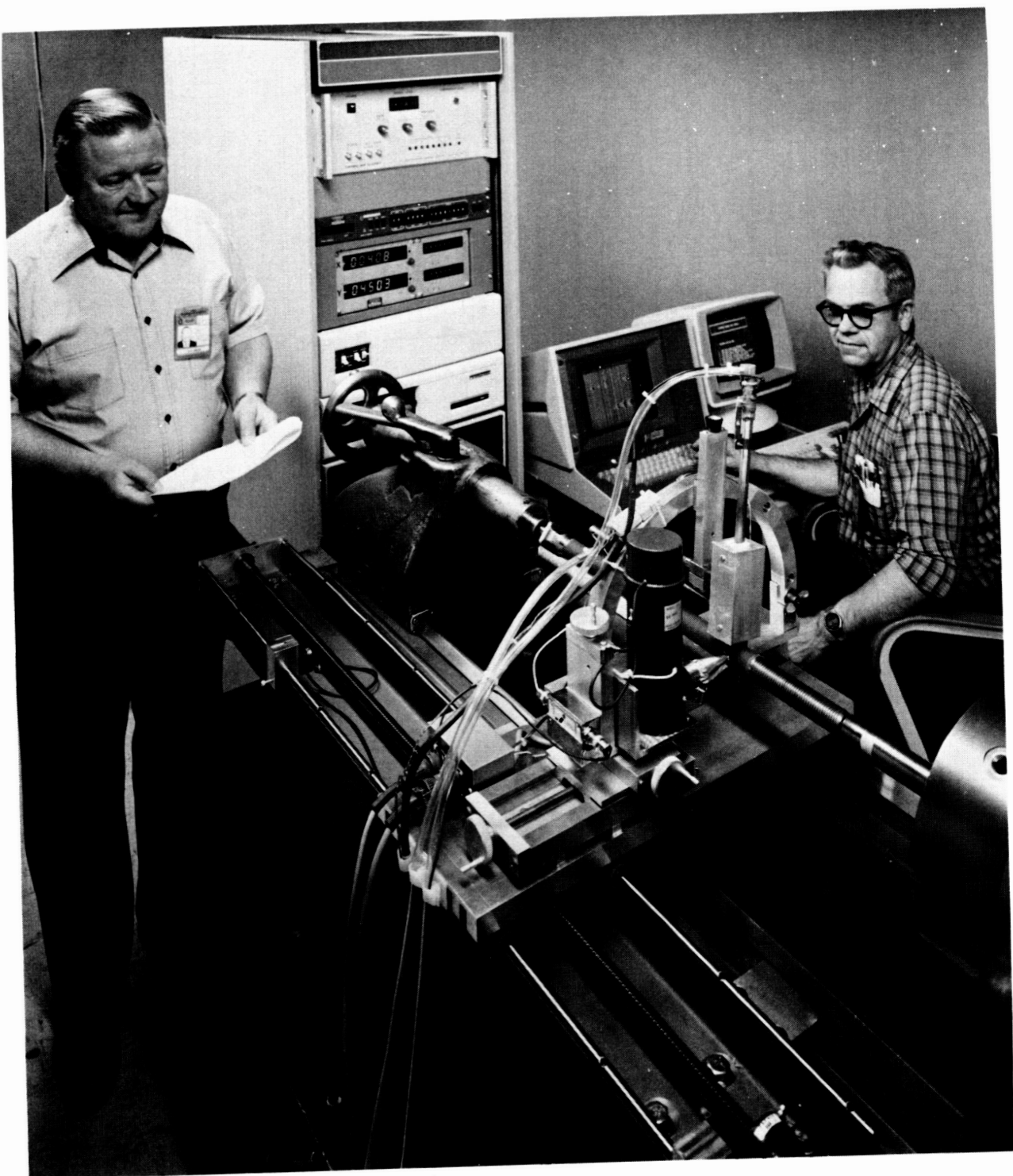
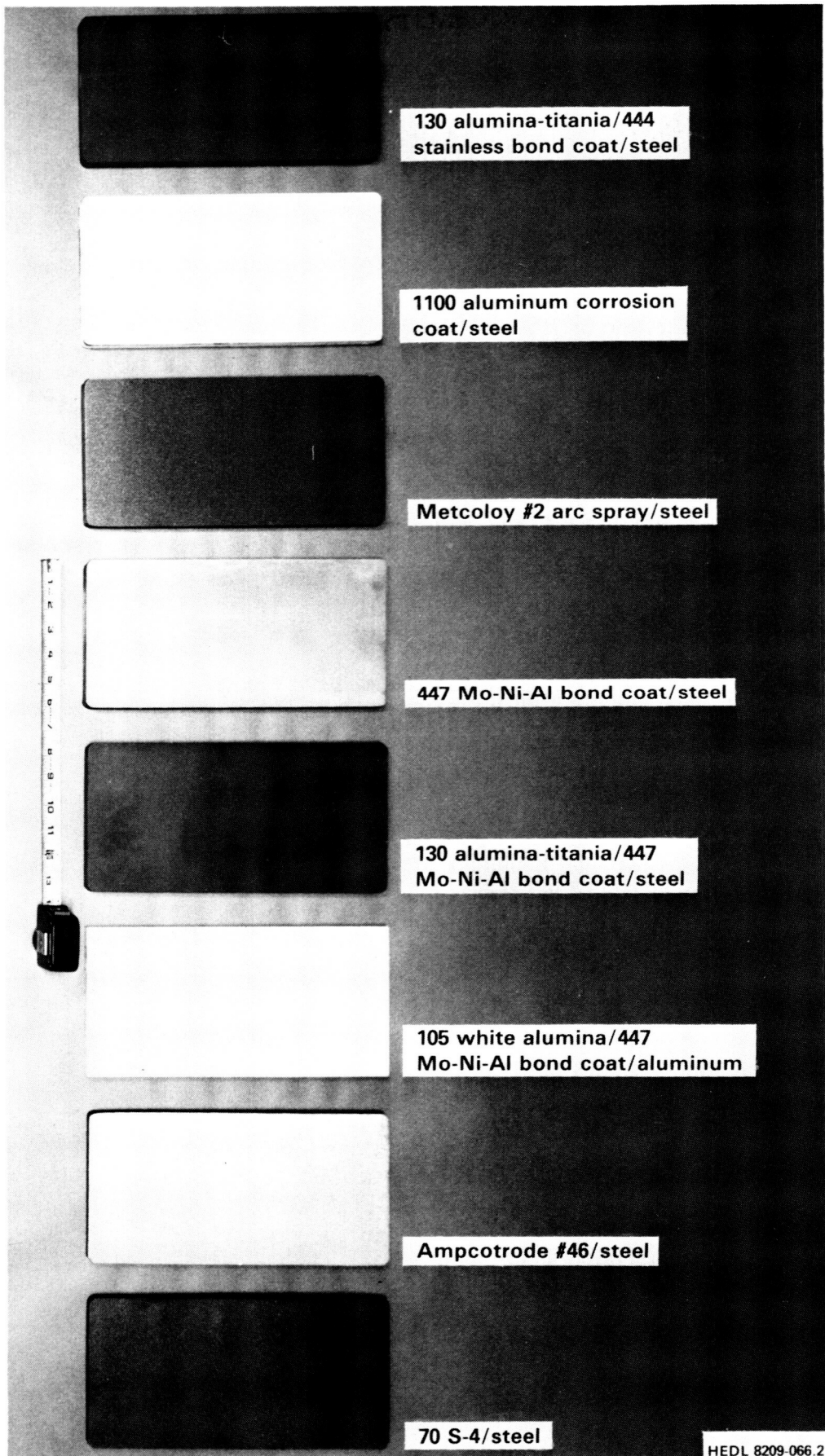


Figure 14.

ORIGINAL PAGE IS
OF POOR QUALITY.

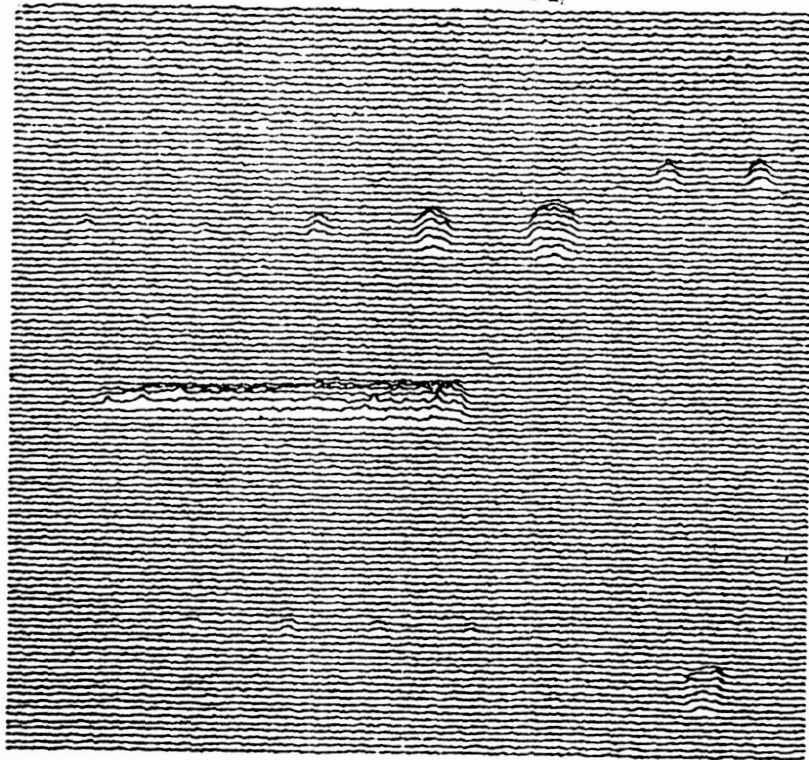




HEDL 8209-066.2

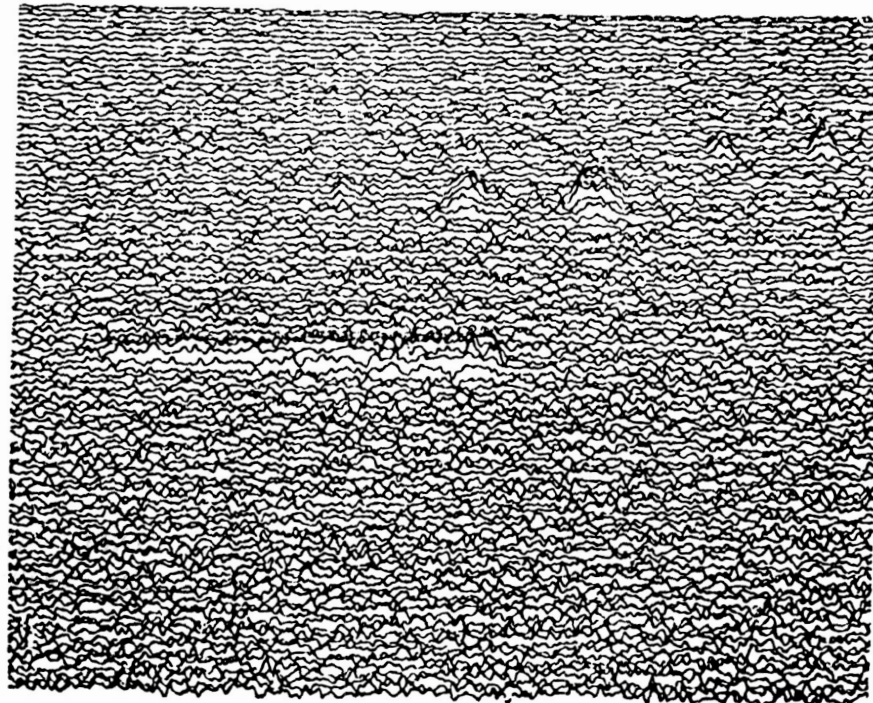
Figure 16.

ORIGINAL PAGE IS
DE POOR QUALITY.



EMISSIVITY INDEPENDENT INFRARED-THERMAL SCAN RESULT SHOWING ALL NONBONDS IN SIDE #1 OF PSNS CYLINDRICAL THERMAL SPRAYED TEST SPECIMEN #11.

Figure 17.



ORDINARY EMISSIVITY DEPENDENT INFRARED-THERMAL SCAN RESULTS ON SIDE #1 OF PSNS CYLINDRICAL THERMAL SPRAYED TEST SPECIMEN #11.
NOTE THAT MOST 1/8 INCH DIAMETER NON-BOND INDICATIONS ARE HIDDEN IN THE BACKGROUND EMISSIVITY VARIATIONS.

Figure 18.

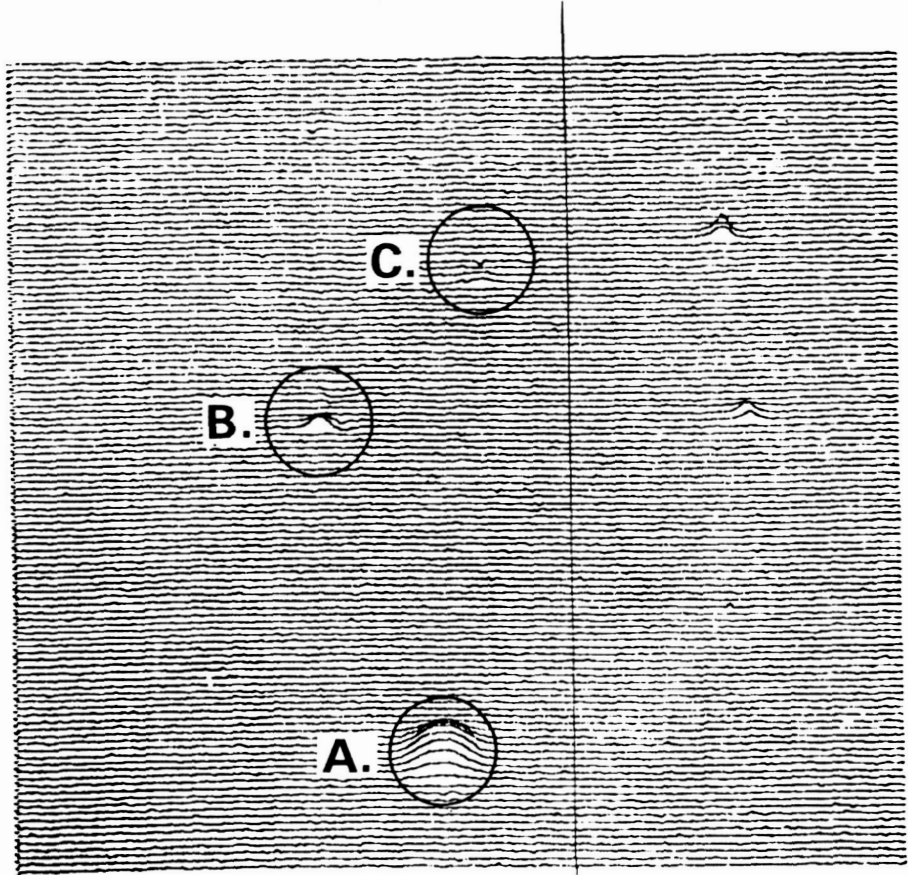


Figure 19.

ORIGINAL PAGE IS
OF POOR QUALITY.

ORIGINAL PAGE IS
OF POOR QUALITY

50X DEFECT "A"

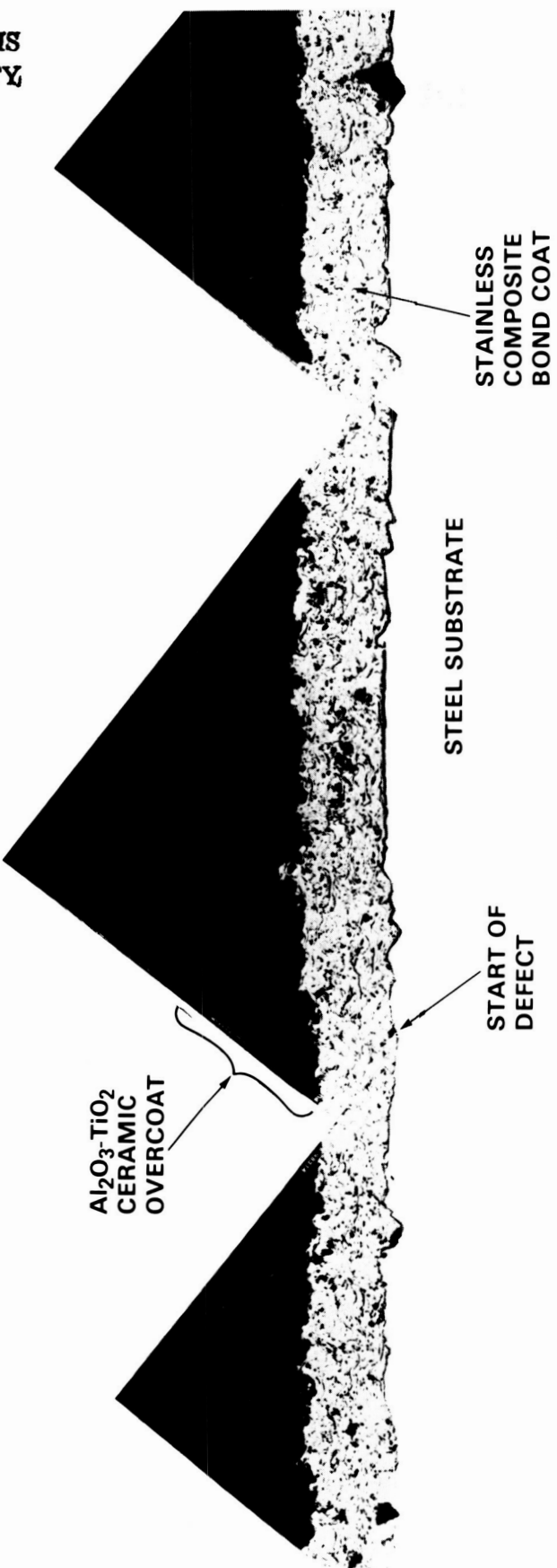


Figure 20.

50X DEFECT "B" LENGTH 3/16 in.

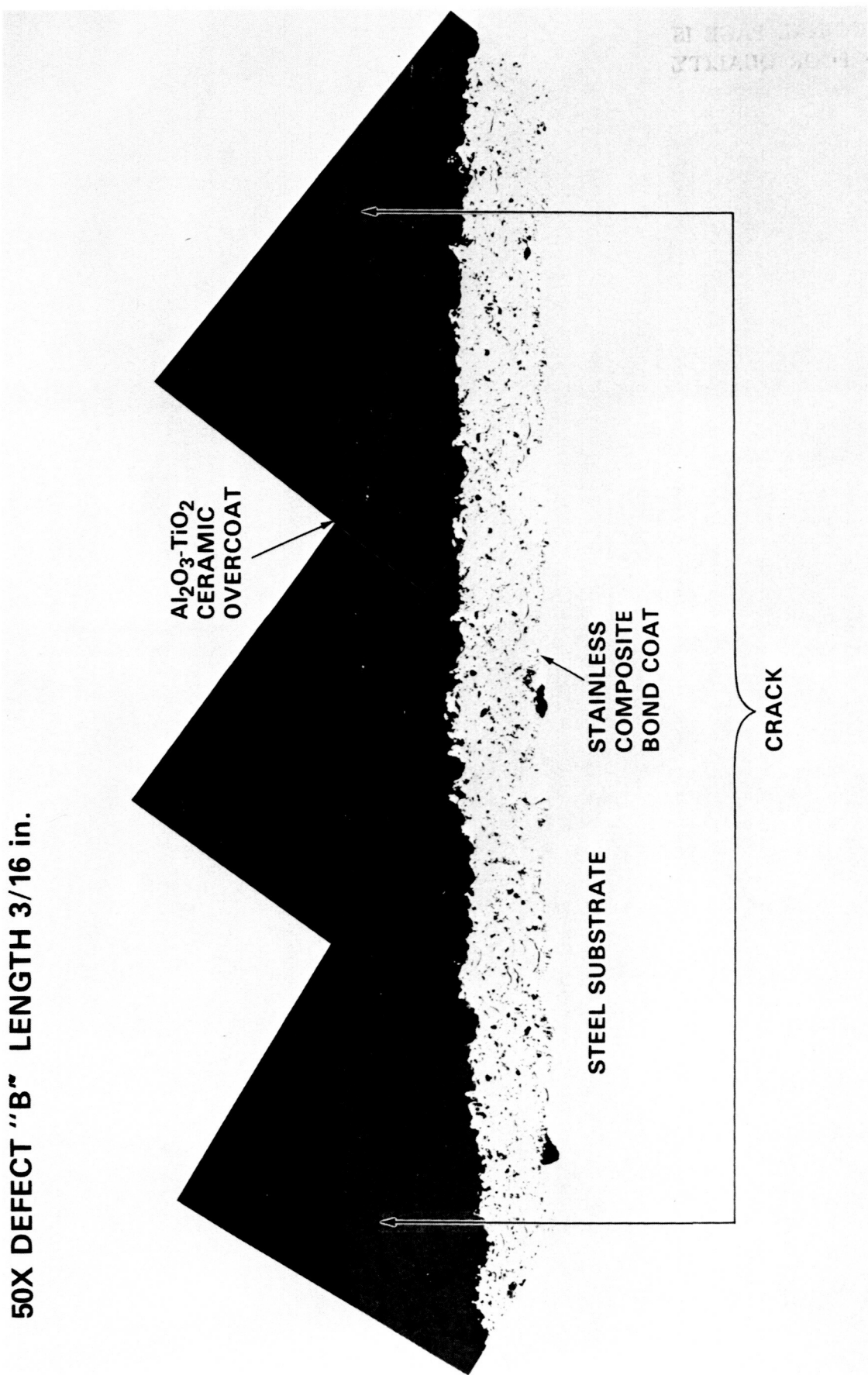


Figure 21.

ORIGINAL PAGE IS
OF POOR QUALITY

DEFECT "C" LENGTH 0.085 in.

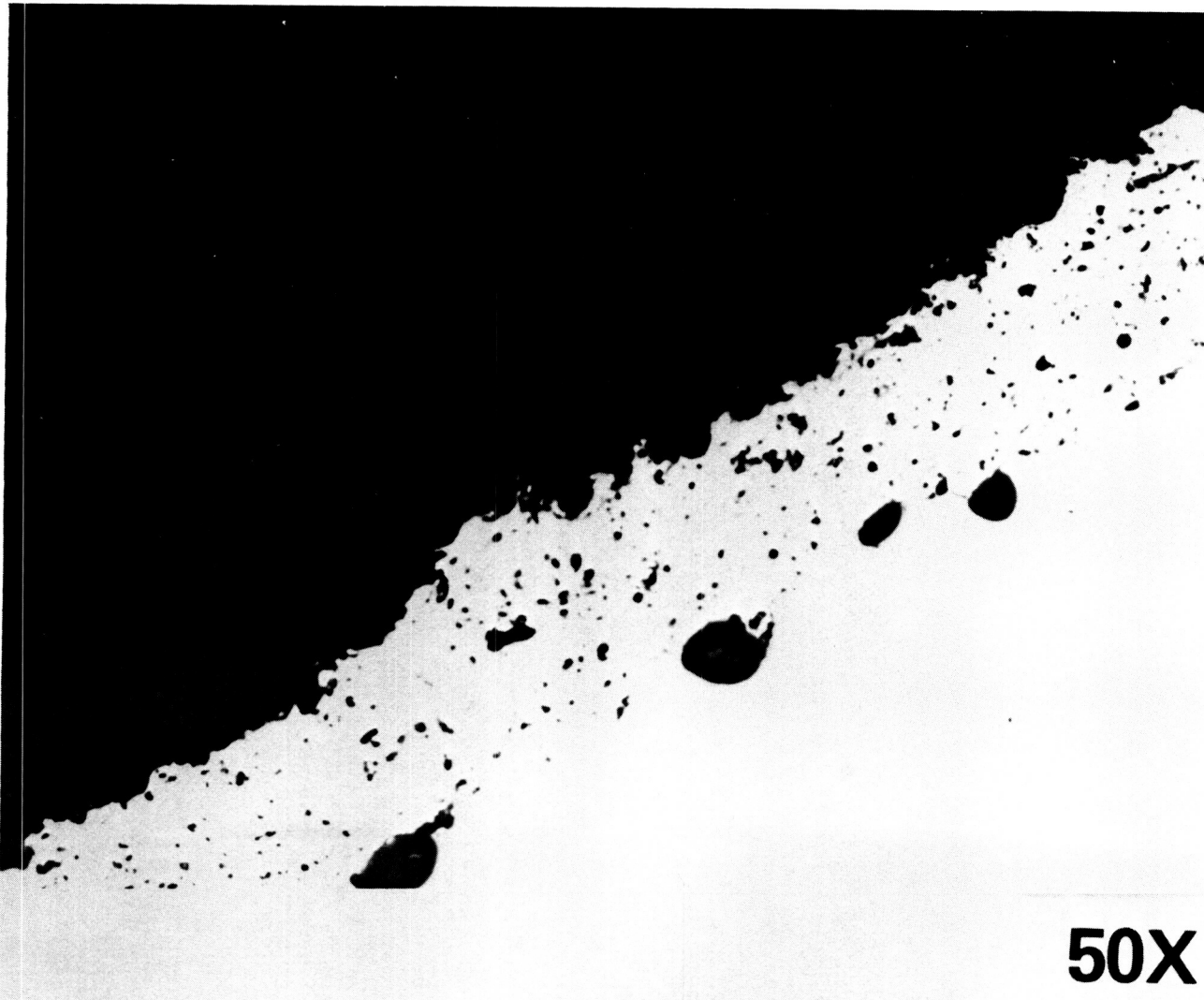


Figure 22.